BNL-98168-2012-JA

INVESTIGATION OF THE RELATIONSHIP BETWEEN HOMOGENEOUS MIXING DEGREE AND TRANSITION SCALE NUMBER WITH THE EXPLICIT MIXING PARCEL MODEL

C. Lu[1, 2], Y. Liu[2], S. Niu[1], S. Krueger[3], and T. Wagner[4]

[1] School of Atmospheric Physics, Key Laboratory of Meteorological Disaster of Ministry of Education, Nanjing University of Information Science and Technology (NUIST), Jiangsu, China 210044
[2] Atmospheric Sciences Division, Brookhaven National Laboratory (BNL), NY, US 11973
[3] Department of Meteorology, University of Utah, Salt Lake City, UT, US 84112
[4] Department of Atmospheric Sciences, Creighton University, Omaha, NE, US, 68178
Corresponding author: Chunsong Lu, Brookhaven National Laboratory, Atmospheric Sciences Division, Building 815E, Upton, NY, USA 11973; luchunsong110@gmail.com

Submitted to Environmental Research Letters

June 2012

Atmospheric Sciences Division/Environmental Sciences Dept.

Brookhaven National Laboratory

U.S. Department of Energy
Office of Science

DISCLAIMER

Abstract

The degree of homogeneous mixing in clouds is critical for improving cloud-related parameterizations in large scale models, but poorly understood and quantified. This study examines various microphysical measures of homogeneous mixing degree and their relationships to entrainment-mixing dynamics as measured by transition scale numbers using the Explicit Mixing Parcel Model (EMPM). Three different measures for the homogeneous mixing degree are newly defined and each is coupled with one of two different transition scale numbers. It is found that all the combinations show positive correlated relationships, with the tightest relationship between the measure of homogeneous mixing degree considering adiabatic number concentration and the transition scale number accounting for mixing fraction of dry air. A parameterization of the entrainment-mixing processes is advanced according to the relationships of homogeneous mixing degree measures to transition scale numbers.

Key words: entrainment-mixing process, homogeneous mixing degree, transition scale number, model

1. Introduction

Turbulent entrainment-mixing processes are critical to many outstanding issues related to clouds, including aerosol indirect effects, cloud-climate feedbacks, warm-rain initiation and remote sensing retrieval of cloud microphysical properties (Paluch and Baumgardner 1989, Yum 1998, Ackerman *et al* 2004, Kim *et al* 2008, Liu *et al* 2008, Del Genio and Wu 2010, Lu *et al* 2011). Several different entrainment-mixing mechanisms have been proposed that may result in different cloud microphysical properties. Consider the homogeneous/inhomogeneous mixing model pioneered by Baker and Latham (1979) and Baker *et al* (1980) for example. In the homogeneous mixing scenario, all droplets evaporate simultaneously; in the extreme inhomogeneous mixing scenario, some droplets evaporate completely while the rest of droplets don't evaporate at all. Although the conceptual model is well established, many quantitative details remain elusive, hindering accurate representation of entrainment-mixing processes and their various effects in atmospheric models. For example, Lasher-Trapp *et al* (2005) found more large droplets were produced in a three-dimensional cloud model assuming inhomogeneous mixing than assuming homogeneous mixing. Using large eddy simulation, Chosson *et al* (2007) found cloud albedo bias changed from -3% to -31% when assuming both mixing mechanisms alternatively in a fragmented and thin stratocumulus cloud. Similarly, with a cloud resolving model, Grabowski (2006) found that the amount of solar energy reaching the surface was the same in the pristine case assuming the homogeneous mixing scenario and in the polluted case with the extreme inhomogeneous mixing; the same conclusion was also reported by Slawinska *et al* (2008) using large eddy simulations with a one-moment microphysics scheme. Although later Morrison and Grabowski (2008), Hill *et al* (2009)

and Slawinska *et al* (2012) found significantly reduced effect of mixing mechanisms in simulations, Morrison and Grabowski (2008) and Hill *et al* (2009) pointed out the effect of mixing mechanisms could be more significant over the entire cloud life cycle, especially during dissipation of clouds. Therefore, it is critical to distinguish homogeneous and inhomogeneous mixing.

Furthermore, the real entrainment-mixing mechanism often falls between the above two extremes (Andrejczuk *et al* 2009, Lu *et al* 2011), posing additional needs for quantifying and parameterizing the degree of homogeneous mixing. This paper is motivated by such needs, focusing on the measure of homogeneous mixing degree, transition scale number (Lu *et al* 2011), and their relationships.

2. Homogeneous Mixing Degree and Transition Scale Number

2.1 Microphysical Measures of Homogeneous Mixing Degree

The diagrams of volume-mean radius (r_v) vs. number concentration (N), r_v^3 vs. N and r_v^3/r_{va}^3 vs. N/N_a (r_{va} and N_a are adiabatic volume mean radius and number concentration, respectively) have been widely used to study homogeneous/inhomogeneous entrainment-mixing mechanisms (Burnet and Brenguier 2007, Lehmann *et al* 2009, Lu *et al* 2011). Based on the diagram of r_v^3/r_{va}^3 vs. N/N_a, we can define three measures of homogeneous mixing degree.

The first measure of homogenous mixing degree (ψ_1) is defined with the help of Figure 1. Similar to Figure 5 in Krueger (2008), Figure 1 conceptually illustrates the sequence of states involved in an entrainment and isobaric mixing event in the EMPM. The states are numbered from 1 to 3. State 1 is an adiabatic cloud, which has an adiabatic

number concentration of N_a and a volume mean radius of r_{va}. State 2 is just after entrainment but before evaporation, which has N_h and r_{va}. From States 2 to 3, mixing and evaporation occur; the number concentration and volume mean radius become N and r_v, respectively, after mixing and evaporation. The extreme inhomogeneous and homogeneous mixing scenarios are denoted by 3' and 3'', respectively. The angle between the line linking States 2 and 3'' and the extreme inhomogeneous mixing line is $\pi/2$; the angle between the line linking States 2 and 3 and the extreme inhomogeneous mixing line is β. As an example, liquid water content is assumed to decrease to be 0.2 of the adiabatic value.

A trigonometrical analysis relates β to the slope of the line linking States 2 and 3:

$$\beta = \tan^{-1}\left(\frac{\frac{r_v^3}{r_{va}^3} - 1}{\frac{N}{N_a} - \frac{N_h}{N_a}}\right), \quad (1)$$

Normalizing β by $\pi/2$ gives the first measure of homogeneous mixing degree:

$$\psi_1 = \frac{\beta}{\pi/2}. \quad (2)$$

Obviously, ψ_1 is between 0 and 1 and measures the degree of homogeneous mixing: a larger ψ_1 indicates a higher degree of homogeneous mixing, with $\psi_1 = 1$ for homogeneous mixing, $\psi_1 = 0$ for extreme inhomogeneous mixing.

The second measure of homogeneous mixing degree (ψ_2) is illustrated with Figure 2. When a mixing process is homogeneous, the number concentration and volume mean radius are N_h and r_{vh}, respectively; when a mixing process is extreme inhomogeneous, the number concentration and volume mean radius are N_i and r_{va}, respectively. In reality, the mixing scenario is between the two extremes with number concentration of N and volume

mean radius of r_v. The second measure of homogeneous mixing degree is expressed as:

$$\psi_2 = \frac{1}{2}\left(\frac{N - N_i}{N_h - N_i} + \frac{r_v^3 - r_{va}^3}{r_{vh}^3 - r_{va}^3}\right), \tag{3}$$

where

$$r_{vh}^3 = \frac{N}{N_h} r_v^3, \tag{4}$$

$$N_i = \frac{r_v^3}{r_{va}^3} N. \tag{5}$$

The third measure of homogeneous mixing degree (ψ_3) can be defined by recognizing that the logarithm operation linearizes the nonlinear r_v^3/r_{va}^3-N/N_a relation such that

$$\psi_3 = \frac{\ln N - \ln N_i}{\ln N_h - \ln N_i} = \frac{\ln r_v^3 - \ln r_{va}^3}{\ln r_{vh}^3 - \ln r_{va}^3}. \tag{6}$$

In a numerical study, Morrison and Grabowski (2008) introduced an empirical parameter to quantify the homogeneous degree such that

$$N = N_0 \left(\frac{q}{q_0}\right)^{\alpha}, \tag{7}$$

where N_0 and q_0 are number concentration and liquid water mixing ratio after entrainment but before evaporation, respectively; N_0 is identical to N_h in Eq. (3); N and q are final number concentration and liquid water mixing ratio, respectively, after mixing and evaporation. These two properties are taken as the values after new saturation is achieved. It can be shown that ψ_3 is uniquely related to α by:

$$\psi_3 = 1 - \alpha, \tag{8}$$

Note that Morrison and Grabowski (2008) assumed a constant α, instead of examining the link between α and microphysical relationships.

2.2 Transition Scale Numbers

The transition scale number is a dynamical measure of the occurrence probability of homogeneous or inhomogeneous entrainment-mixing process (Lu *et al* 2011); the larger the N_L, the stronger the homogenous entrainment-mixing process and the weaker the inhomogeneous entrainment-mixing process. N_L is calculated as the ratio of transition length (L^*) introduced by Lehmann *et al* (2009) to the Kolmogorov microscale (η):

$$N_L = \frac{L^*}{\eta} = \frac{\varepsilon^{1/2}\tau^{3/2}_{\text{react}}}{\eta}, \tag{9}$$

where ε is eddy dissipation rate. η is given by

$$\eta = \left(\frac{\nu^3}{\varepsilon}\right)^{1/4}, \tag{10}$$

where v is the kinematic viscosity (Wyngaard 2010). τ_{react} is defined as either the time when the droplets have completely evaporated or the time at which the relative humidity has reached 99.5% (s > -0.005, Lehmann *et al* 2009); τ_{react} is calculated by the equations below:

$$\frac{dr}{dt} = A\frac{s}{r}, \tag{11a}$$

$$\frac{ds}{dt} = -Brs, \tag{11b}$$

where r is cloud droplet radius, s supersaturation, A a function of pressure and temperature, and B a function of pressure, temperature and proportional to cloud droplet number concentration (Rogers and Yau 1989). If N_a is used in B, scale number is denoted by N_{La}; while if N_0 is used, scale number is denoted by N_{L0}. For a group of droplets, r in the above equations is replaced with r_{va}.

3. Relationship between Homogeneous Mixing Degree and Transition Scale Number

Since both ψ and N_L describe the possibility of homogeneous mixing processes, they are expected to have a positive relationship theoretically. Due to the difficulty in accurately obtaining cloud base in aircraft observations (e.g., Vogelmann *et al* 2012), the properties needed in the calculations of ψ and N_L (e.g., N_h, q_0, r_{vh}) could have large unknown uncertainties. The EMPM does not suffer from this problem because the cloud base height is an input parameter; thus the relationship between ψ and N_L is explored using the EMPM model below.

3.1 Model Description and Simulation Parameters

The EMPM model was developed by Krueger *et al* (1997); Su *et al* (1998) further included individual droplet growth in the model. The model depicts the fine-scale internal structure of a rising parcel using a 1D domain. The internal structure evolves in the model as a consequence of discrete entrainment events and explicit turbulent mixing based on the linear eddy model developed by Kerstein (1988, 1992). As summarized in Krueger (2008), the model works as follows. First, the parcel ascends adiabatically above cloud base, while the droplets grow by condensation. Second, when entrainment occurs, the subsaturated entrained air replaces a same-sized segment of the cloudy parcel. Third, the

cloudy air and the newly entrained air undergo a finite rate turbulent isobaric mixing process, during which many droplets encounter the entrained subsaturated air, resulting in partial or even total evaporation of some droplets.

Table 1 summarizes the input parameters of the model. In this study, the cloud base and environmental information are taken from Hawaiian trade cumulus cloud measurements (Raga *et al* 1990). The cloud base pressure, temperature and water vapor mixing ratio are 964.0 hPa, 293.6 K and 15.7 g kg^{-1}, respectively. N_a is 102.7 cm^{-3}; these droplets are randomly assigned to the 20 m × 0.001 m × 0.001 m model domain. The entrainment level is set at the pressure of 888.9 hPa where the temperature and relative humidity in the entrained air are 289.3 K and 88%, respectively. Updraft is set to be a constant, 2 m s^{-1}, before the entrainment level; after that the parcel stops rising and isobaric mixing occurs. The grid size is set to be 0.0017 m.

To explore the relationship between the homogeneous mixing degree and the transition scale number, we perform a suite of simulations with different combinations of model parameters: N_a is set to be 102.7, 205.4, 308.1, 410.8 and 513.5 cm^{-3}; relative humidity (RH) is set to be 11%, 22%, 44%, 66% and 88%; ε is set to be 1×10^{-5}, 5×10^{-4}, 1×10^{-3}, 5×10^{-3}, 1×10^{-2} and 5×10^{-2} m^2s^{-3}; blob number is set to be 2 - 9 and the entrained blob size is 2 m × 0.001 m × 0.001 m; so mixing fraction of dry air is 0.2 - 0.9. When blob number is 1, mixing fraction of dry air is small and volume-mean radius increases due to residual supersaturation; to minimize this effect and focus on the entrainment-mixing processes, the blob number starts from 2.

3.2 Results

Figure 3 compares the relationships of homogeneous mixing degree measures (ψ_1, ψ_2, ψ_3) to the transition scale numbers (N_{La}, N_{L0}). In every entrainment and isobaric mixing process, liquid water mixing ratio decreases sharply. When liquid water mixing ratio does not decrease for 15 s, it is assumed that new saturation is achieved; the N and r_v in the domain are considered to be the final values used in the calculations of ψ_1, ψ_2 and ψ_3. In some sensitivity tests, clouds completely evaporate due to the large mixing fraction of dry air and/or low relative humidity (e.g., mixing fraction of dry air from 0.3 to 0.9, RH = 11%); these cases are not included in Figure 3. Positive relationships between the three measures of homogeneous mixing degree and the scale numbers are found in two regimes: RH = 11%, 22%, 44% and 66% and RH = 88%. The reason for the two regimes is that different conditions are satisfied in solving Eq. (11) to obtain τ_{react} and then N_L; for RH = 11%, 22%, 44% and 66% and for RH = 88%, the first condition "droplets have completely evaporated" and the second condition "relative humidity has reached 99.5%" are satisfied, respectively. For RH = 88%, all ψ_1, ψ_2 and ψ_3 are close to 100%; it is not important to distinguish homogeneous and inhomogeneous mixing when entrained dry air has a high relative humidity (Lehmann *et al* 2009, Devenish *et al* 2012, Slawinska *et al* 2012). Thus we will focus on the regime with RH = 11%, 22%, 44% and 66%; the best fit lines are also shown in Figure 3.

As shown in Figure 3, ψ_2 vs. N_L and ψ_3 vs. N_L are close to each other, while ψ_1 vs. N_L has the tightest relationship. A tight relationship is important for a parameterization; thus it is suggested to use ψ_1 if N_a is available [N_a is necessary in Eq. (1)], otherwise, use ψ_2 or ψ_3. Figure 3 also shows that the relationships of ψ_1, ψ_2 and ψ_3 to N_{L0} are tighter than those of ψ_1, ψ_2 and ψ_3 to N_{La}, which is especially true for ψ_2 and ψ_3. To figure out the reasons,

Figure 4 compares ψ_3 vs. N_{La} and ψ_3 vs. N_{L0} with a mixing fraction of dry air changing from 0.2 to 0.5; others being equal, the ψ_3 is smaller with a larger mixing fraction of dry air; for example, ψ_3 decreases from "1" to "2" or from "I" to "II". This is consistent with observations in cumuli analyzed by Burnet and Brenguier (2007); they found that mixing approached the homogeneous type when mixing fraction of dry air was small and approached the inhomogeneous type when mixing fraction of dry air was large. Similar conclusion can also be drawn from Figure 5a and 5b in Lehmann *et al* (2009). Other studies have also proven that mixing fraction of dry air is critical for mixing processes (Jensen and Baker 1989, Hicks *et al* 1990, Schlüter 2006, Jeffery 2007). N_{La} cannot reflect the role of dry air mixing fraction but N_{L0} can. The reason is for N_{La}, the number concentration used in the calculation of B in Eq. (11) is the adiabatic number concentration which is independent of mixing fraction; as for N_{L0}, the number concentration used is the number concentration just after entrainment, which considers the mixing fraction. As a result, the change from "I" to "II" is along a vertical line while that from "1" to "2" is toward the bottom left corner of Figure 4, causing less dispersion. Thus it is suggested to use N_{L0} instead of N_{La} in the future studies. Additionally, N_{L0} can be combined with a new approach for estimating entrainment rate developed by Lu *et al* (2012), facilitating a straightforward connection between the two sides of entrainment-mixing processes (homogeneous/inhomogeneous entrainment-mixing mechanisms and entrainment rate estimation), because N_{L0} and the new approach are both related to mixing fraction of dry air.

Although the relationships are tighter with N_{L0}, dispersion of the data points in Figure 3 still exists. To further determine the influencing factors, the effects of dissipation rate,

relative humidity, adiabatic number concentration and mixing fraction of dry air are examined. As exemplified in Figure 5, in every group (e.g., "ψ_1 vs. N_{L0}, RH = 11%" in Figure 5a), the dissipation rates of the six data points from left to right are 1×10^{-5}, 5×10^{-4}, 1×10^{-3}, 5×10^{-3}, 1×10^{-2} and 5×10^{-2} m^2s^{-3}, respectively. Smaller dissipation rates correspond to smaller homogeneous mixing degree values, because a smaller dissipation rate means a slower mixing process, which is favorable for inhomogeneous mixing process (e.g., Baker *et al* 1984). Comparison of the results with RH = 66% and 11% shows that lower RH causes smaller ψ and a larger slope of ψ vs. N_{L0} (Figure 5a); lower RH means faster evaporation of droplets, making mixing more likely inhomogeneous (e.g., Siebert *et al* 2006). Figure 5b shows that ψ is smaller for a larger adiabatic droplet number concentration, because a larger adiabatic number concentration causes smaller droplets, increasing the likelihoods of complete evaporation and extreme inhomogeneous mixing (e.g., Hill *et al* 2009). As discussed above, larger mixing fraction of dry air causes more inhomogeneous mixing, i.e., smaller ψ (Figures 4, 5c). These factors altogether affect the relationships between the homogeneous mixing degree and the scale number.

4. Summary

The Explicit Mixing Parcel Model is employed to investigate the relationship between the homogeneous mixing degree and the transition scale number. Three measures of homogeneous mixing degree are newly defined and two transition scale numbers are used. As theoretically expected, the three homogeneous mixing degrees are

all positively related to the two scale numbers. Among the three measures of homogeneous mixing degree, it is suggested to use ψ_1 if N_a is available because ψ_1 has the tightest relationship with the two scale numbers; otherwise, use ψ_2 or ψ_3 instead. As to transition scale numbers, it is suggested to use N_{L0} instead of N_{La} in the future studies of entrainment-mixing processes because the relationships of N_{L0} to the three homogeneous mixing degree measures are tighter than the relationships of N_{La} to the three measures. The reason is that N_{L0} considers mixing fraction of dry air while N_{La} does not. Besides the advantage of N_{L0} shown here, the combination of N_{L0} and a new entrainment rate estimation approach (Lu *et al* 2012) presents a potential to link the two sides of entrainment-mixing processes (homogeneous/inhomogeneous entrainment-mixing mechanisms and entrainment rate estimation).

The relationship between the homogeneous mixing degree and transition scale number also suggests a new parameterization for entrainment-mixing processes in models with two-moment microphysical schemes. The transition scale number can be calculated from the microphysical properties (r_{va} and N_a or N_0) and meteorological elements before entrainment-mixing processes for every cloud grid at every time step in models; the degree of homogeneous mixing can be estimated from the transition scale number based on the best fit lines in Figure 3; with the homogeneous mixing degree and Eq. (2), (3) or (6), the values of N and r_v after the entrainment-mixing processes can be calculated.

Acknowledgment

We thank Satoshi Endo at the Brookhaven National Lab for many useful discussions on this manuscript. Liu and Lu were supported by the Department of Energy (DOE)

Earth System Modeling (ESM) program via the FASTER project (www.bnl.gov/esm) and Atmospheric System Research (ASR) program. Niu was supported by the Qing-Lan Project for Cloud-Fog-Precipitation-Aerosol Study in Jiangsu Province, China, a Project Funded by the Priority Academic Program Development of Jiangsu Higher Education Institutions. The development of the EMPM was supported by the Office of Naval Research under Grant N00014-91-J-1175.

References

Ackerman A S, Kirkpatrick M P, Stevens D E and Toon O B 2004 The impact of humidity above stratiform clouds on indirect aerosol climate forcing *Nature* 432 1014-1017

Andrejczuk M, Grabowski W W, Malinowski S P and Smolarkiewicz P K 2009 Numerical simulation of cloud–clear air interfacial mixing: Homogeneous versus inhomogeneous mixing *J. Atmos. Sci.* 66 2493-2500

Baker M B, Breidenthal R E, Choularton T W and Latham J 1984 The effects of turbulent mixing in clouds *J. Atmos. Sci.* 41 299-304

Baker M B, Corbin R G and Latham J 1980 The influence of entrainment on the evolution of cloud droplet spectra: I. A model of inhomogeneous mixing *Q. J. Roy. Meteor. Soc.* 106 581-598

Baker M B and Latham J 1979 The evolution of droplet spectra and the rate of production of embryonic raindrops in small cumulus clouds *J. Atmos. Sci.* 36 1612-1615

Burnet F and Brenguier J L 2007 Observational study of the entrainment-mixing process in warm convective clouds *J. Atmos. Sci.* 64 1995-2011

Chosson F, Brenguier J-L and Schüller L 2007 Entrainment-mixing and radiative transfer simulation in boundary layer clouds *J. Atmos. Sci.* 64 2670-2682

Del Genio A D and Wu J 2010 The role of entrainment in the diurnal cycle of continental convection *J. Climate* 23 2722-2738

Devenish B J *et al* 2012 Droplet growth in warm turbulent clouds *Q. J. Roy. Meteor. Soc.* (In press)

Grabowski W W 2006 Indirect impact of atmospheric aerosols in idealized simulations of convective-radiative quasi equilibrium *J. Climate* 19 4664-4682

Hicks E, Pontikis C and Rigaud A 1990 Entrainment and mixing processes as related to droplet growth in warm midlatitude and tropical clouds *J. Atmos. Sci.* 47 1589-1618

Hill A A, Feingold G and Jiang H 2009 The influence of entrainment and mixing assumption on aerosol-cloud interactions in marine stratocumulus *J. Atmos. Sci.* 66 1450-1464

Jeffery C A 2007 Inhomogeneous cloud evaporation, invariance, and Damköhler number *J. Geophys. Res.* 112 D24S21

Jensen J B and Baker M B 1989 A simple model of droplet spectral evolution during turbulent mixing *J. Atmos. Sci.* 46 2812-2829

Kerstein A R 1988 A linear-eddy model of turbulent scalar transport and mixing *Combust. Sci. Technol.* 60 391-421

Kerstein A R 1992 Linear-eddy modelling of turbulent transport. Part 7. Finite-rate chemistry and multi-stream mixing *J. Fluid Mech.* 240 289-313

Kim B-G, Miller M A, Schwartz S E, Liu Y and Min Q 2008 The role of adiabaticity in the aerosol first indirect effect *J. Geophys. Res.* 113 D05210

Krueger S, Su C and McMurtry P 1997 Modeling entrainment and finescale mixing in cumulus clouds *J. Atmos. Sci.* 54 2697-2712

Krueger S K 2008 Fine-scale modeling of entrainment and mixing of cloudy and clear air, *Proc. the 15th International Conference on Clouds and Precipitation (Cancun, Mexico)*

Lasher-Trapp S G, Cooper W A and Blyth A M 2005 Broadening of droplet size distributions from entrainment and mixing in a cumulus cloud *Q. J. Roy. Meteor. Soc.* 131 195-220

Lehmann K, Siebert H and Shaw R A 2009 Homogeneous and inhomogeneous mixing in cumulus clouds: dependence on local turbulence structure *J. Atmos. Sci.* 66 3641-3659

Liu Y, Daum P H, Yum S S and Wang J 2008 Use of microphysical relationships to discern growth/decay mechanisms of cloud droplets with focus on Z-LWC relationships, *Proc. 15th International Conference on Clouds and Precipitation (Cancun, Mexico)*

Lu C, Liu Y and Niu S 2011 Examination of turbulent entrainment-mixing mechanisms using a combined approach *J. Geophys. Res.* 116 D20207

Lu C, Liu Y, Yum S S, Niu S and Endo S 2012 A new approach for estimating entrainment rate in cumulus clouds *Geophys. Res. Lett.* 39 L04802

Morrison H and Grabowski W W 2008 Modeling supersaturation and subgrid-scale mixing with two-moment bulk warm microphysics *J. Atmos. Sci.* 65 792-812

Paluch I R and Baumgardner D G 1989 Entrainment and fine-scale mixing in a continental convective cloud *J. Atmos. Sci.* 46 261-278

Raga G B, Jensen J B and Baker M B 1990 Characteristics of cumulus band clouds off the coast of Hawaii *J. Atmos. Sci.* 47 338-356

Rogers R R and Yau M K 1989 *A short course in cloud physics* (Burlington, MA, USA: Butterworth Heinemann) 3rd ed

Schlüter M H 2006 *The effects of entrainment and mixing processes on the droplet size distributions in cumuli* Master thesis University of Utah

Siebert H, Franke H, Lehmann K, Maser R, Wei Saw E, Schell D, Shaw R A and Wendisch M 2006 Probing finescale dynamics and microphysics of clouds with helicopter-borne measurements *B. Am. Meteorol. Soc.* 87 1727-1738

Slawinska J, Grabowski W W, Pawlowska H and Morrison H 2012 Droplet activation and mixing in large-eddy simulation of a shallow cumulus field *J. Atmos. Sci.* 69 444-462

Slawinska J, Grabowski W W, Pawlowska H and Wyszogrodzki A A 2008 Optical properties of shallow convective clouds diagnosed from a bulk-microphysics large-eddy simulation *J. Climate* 21 1639-1647

Su C-W, Krueger S K, McMurtry P A and Austin P H 1998 Linear eddy modeling of droplet spectral evolution during entrainment and mixing in cumulus clouds *Atmos. Res.* 47-48 41-58

Vogelmann A M *et al* 2012 RACORO extended-term, aircraft observations of boundary-layer clouds *B. Am. Meteorol. Soc.* (In press)

Wyngaard J C 2010 *Turbulence in the Atmosphere* (New York: Cambridge University Press)

Yum S 1998 *Cloud droplet spectral broadening in warm clouds: An observational and model study* Ph. D. thesis 191 pp University of Nevada

Caption List

Figure 1. Mixing diagram of the cubic volume mean radius (r_v^3) vs. the droplet number concentration (N) normalized by their adiabatic values, r_{va}^3 and N_a, respectively. The three black solid lines correspond to extreme inhomogeneous mixing, homogeneous mixing, and contour of $\gamma = 0.2$; γ is the ratio of liquid water content (LWC) to its adiabatic value (LWC_a), respectively. This diagram is for the definition of the first homogeneous mixing degree. See text for the meanings of the other lines and symbols.

Figure 2. Same as Figure 1 but for the definition of the second homogeneous mixing degree. See text for the meanings of the other lines and symbols.

Figure 3. The relationships between the three measures of homogeneous mixing degree (ψ_1, ψ_2, ψ_3) and the two scale numbers (N_{La}, N_{L0}), respectively, under all kinds of conditions as listed in Table 1 except the cases where clouds completely dissipate.

Figure 4. The relationships between the homogeneous mixing degree (ψ_3) and the two scale numbers (N_{La}, N_{L0}), respectively, with two mixing fractions of dry air (f) being 0.2 and 0.5. The relative humidity (RH) and adiabatic number concentration (N_a) are 66% and 205.4 cm^{-3}, respectively; in every group (e.g., ψ_3 vs. N_{La}, $f = 0.2$), dissipation rates are 1×10^{-5}, 5×10^{-4}, 1×10^{-3}, 5×10^{-3}, 1×10^{-2} and 5×10^{-2} m^2s^{-3} for the 6 data points (from left to right), respectively.

Figure 5. (a) Relationships between the three measures of homogeneous mixing degree (ψ_1, ψ_2, ψ_3) and the scale number (N_{L0}), respectively, with relative humidity (RH) being 11% and 66%; adiabatic number concentration (N_a) and mixing fraction of dry air (f) are 308.1 cm^{-3} and 0.2, respectively. (b) Relationships between ψ_1, ψ_2, ψ_3 and N_{L0}, respectively, with N_a being 102.7 and 513.5 cm^{-3}; f and RH are 0.4 and 66%, respectively. (c) Relationships between ψ_1, ψ_2, ψ_3 and N_{L0}, respectively, with f being 0.2 and 0.5; RH and N_a are 66% and 102.7 cm^{-3}, respectively. In every group (e.g., ψ_1 vs. N_{L0}, RH = 11%), dissipation rates are 1×10^{-5}, 5×10^{-4}, 1×10^{-3}, 5×10^{-3}, 1×10^{-2} and 5×10^{-2} m^2s^{-3} for the 6 data points (from left to right), respectively.

Table 1. Input parameters for the EMPM model

	Parameters	Values
Cloud base conditions	Cloud base pressure (hPa)	964.0
	Cloud base temperature (K)	293.6
	Cloud base water vapor mixing ratio (g kg^{-3})	15.7
	Adiabatic droplet number concentration, N_a (cm^{-3})	102.7, 205.4, 308.1, 410.8, 513.5
Entrainment conditions	Domain size (m)	20×0.001×0.001
	Entrainment level pressure (hPa)	888.9
	Entrained air temperature (K)	289.3
	Entrained air relative humidity, RH (%)	11%, 22%, 44%, 66%, 88%
	Vertical velocity	Before mixing, 2 m s^{-1}, after mixing, 0 m s^{-1}.
	Grid size (m)	0.0017
	Dissipation rate, ε (m^2s^{-3})	1×10^{-5}, 5×10^{-4}, 1×10^{-3}, 5×10^{-3}, 1×10^{-2}, 5×10^{-2}
	Entrained air blob size (m)	2×0.001×0.001
	Entrained air blob number	2, 3, 4, 5, 6, 7, 8, 9
	Mixing fraction of dry air, f	0.2, 0.3, 0.4, 0.5, 0.6, 0.7, 0.8, 0.9

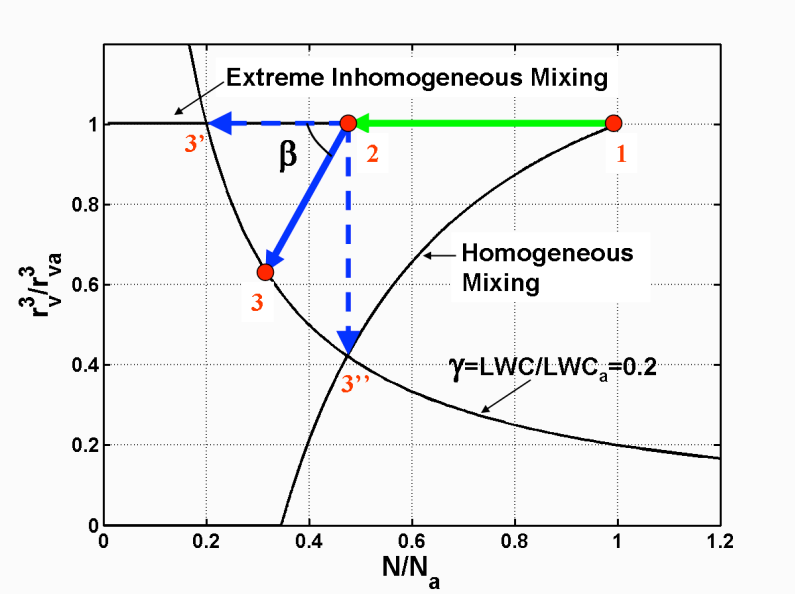

Figure 1. Mixing diagram of the cubic volume mean radius (r_v^3) vs. the droplet number concentration (N) normalized by their adiabatic values, r_{va}^3 and N_a, respectively. The three black solid lines correspond to extreme inhomogeneous mixing, homogeneous mixing, and contour of $\gamma = 0.2$; γ is the ratio of liquid water content (LWC) to its adiabatic value (LWC_a), respectively. This diagram is for the definition of the first homogeneous mixing degree. See text for the meanings of the other lines and symbols.

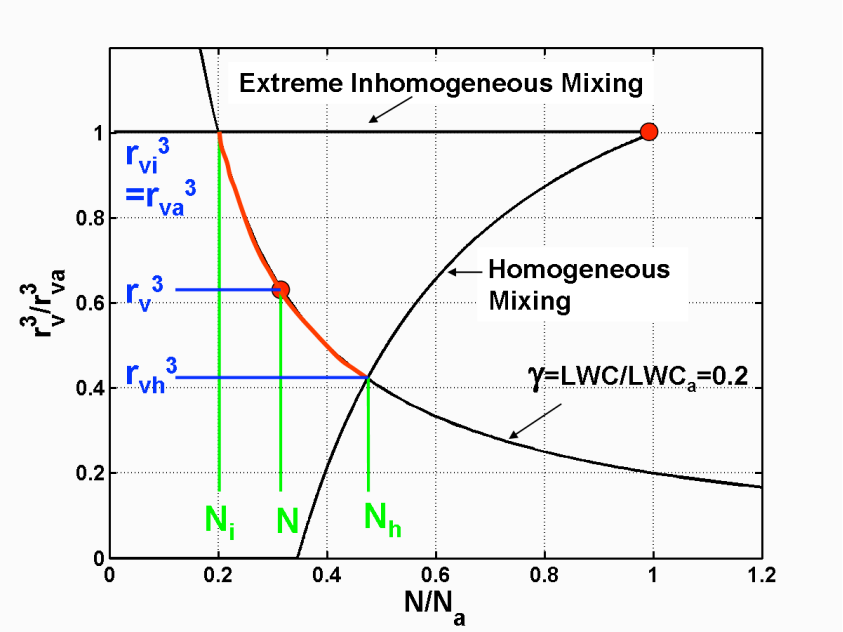

Figure 2. Same as Figure 1 but for the definition of the second homogeneous mixing degree. See text for the meanings of the other lines and symbols.

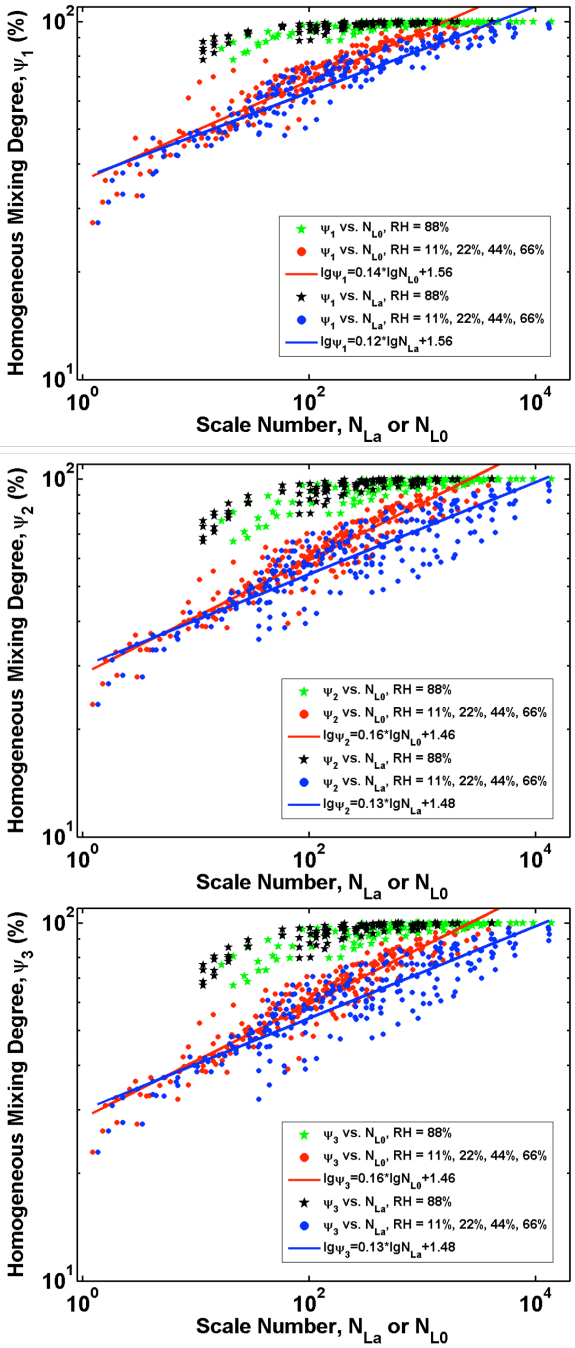

Figure 3. The relationships between the three measures of homogeneous mixing degree (ψ_1, ψ_2, ψ_3) and the two scale numbers (N_{La}, N_{L0}), respectively, under all kinds of conditions as listed in Table 1 except the cases where clouds completely dissipate.

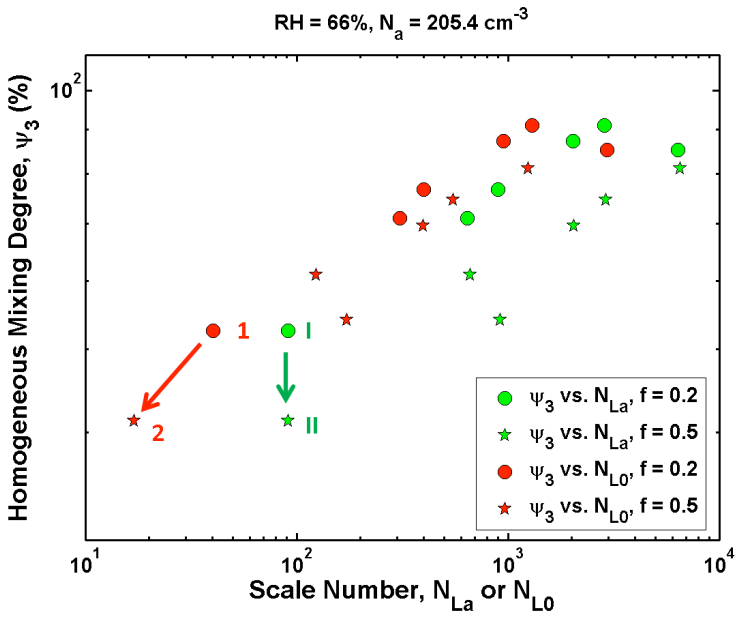

Figure 4. The relationships between the homogeneous mixing degree (ψ_3) and the two scale numbers (N_{La}, N_{L0}), respectively, with two mixing fractions of dry air (f) being 0.2 and 0.5. The relative humidity (RH) and adiabatic number concentration (N_a) are 66% and 205.4 cm^{-3}, respectively; in every group (e.g., ψ_3 vs. N_{La}, f = 0.2), dissipation rates are 1×10^{-5}, 5×10^{-4}, 1×10^{-3}, 5×10^{-3}, 1×10^{-2} and 5×10^{-2} m^2s^{-3} for the 6 data points (from left to right), respectively.

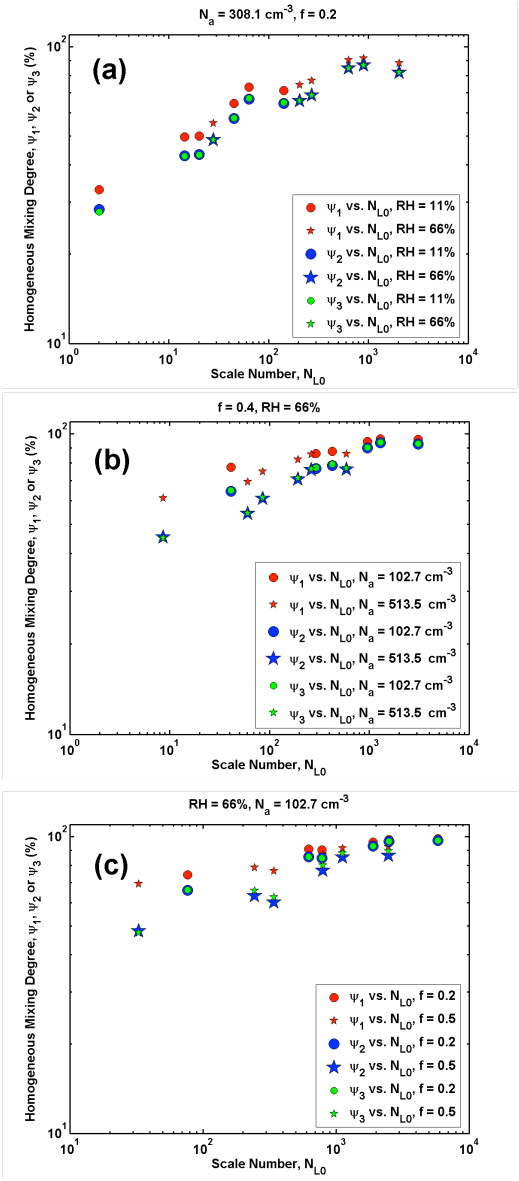

Figure 5. (a) Relationships between the three measures of homogeneous mixing degree (ψ_1, ψ_2, ψ_3) and the scale number (N_{L0}), respectively, with relative humidity (RH) being 11% and 66%; adiabatic number concentration (N_a) and mixing fraction of dry air (f) are 308.1 cm^{-3} and 0.2, respectively. (b) Relationships between ψ_1, ψ_2, ψ_3 and N_{L0}, respectively, with N_a being 102.7 and 513.5 cm^{-3}; f and RH are 0.4 and 66%, respectively. (c) Relationships between ψ_1, ψ_2, ψ_3 and N_{L0}, respectively, with f being 0.2 and 0.5; RH and N_a are 66% and 102.7 cm^{-3}, respectively. In every group (e.g., ψ_1 vs. N_{L0}, RH = 11%), dissipation rates are 1×10^{-5}, 5×10^{-4}, 1×10^{-3}, 5×10^{-3}, 1×10^{-2} and 5×10^{-2} m^{2}s^{-3} for the 6 data points (from left to right), respectively.